2012 Intelligent Vehicles Symposium
Alcalá de Henares, Spain, June 3-7, 2012

Manual convoying of automated urban vehicles relying on monocular vision

P. Avanzini[1,3], B. Thuilot[1,3] and P. Martinet[2,3]

[1] Clermont Université, Université Blaise Pascal, Institut Pascal, BP 10448, 63000 Clermont-Ferrand, France
[2] IRCCYN, Ecole Centrale de Nantes, 1 rue de la Noé, BP 92101, 44321 Nantes Cedex 03, France
[3] CNRS, UMR 6602, Institut Pascal, 63177 Aubière, France
Pierre.AVANZINI@lasmea.univ-bpclermont.fr

Abstract— **This paper deals with platooning navigation in the context of innovative solutions for urban transportation systems. More precisely, the case of a manually driven vehicle leading a convoy of automated ones is considered. Vehicle localization relies solely on monocular vision: a 3D map of the environment is built beforehand from reference video sequences, and then used to derive vehicle absolute location from the current camera image. The 3D vision map presents however distortions w.r.t. a metric world, but these latter can be shown to be locally homogeneous. They can then be accurately corrected via a 1-dim. function evaluated with a nonlinear observer relying on odometric data. Next, the platoon reference trajectory is built as a B-Spline curve extended on-line via local optimization from the successive locations of the lead vehicle, and a global decentralized control strategy, supported by inter-vehicle communication, is designed to achieve accurate platooning with no oscillation within the convoy. Experimental results, carried out with two urban vehicles, demonstrate the capabilities of the proposed approach.**

Index Terms— **automatic guided vehicles, platooning, nonlinear control, monocular vision, trajectory generation.**

I. INTRODUCTION

Reducing congestion in metropolitan areas is a critical goal to be currently addressed in a sustainable perspective. When public demand is properly structured, as within inner-cities or large industrial areas, autonomous electric vehicles available in free-access constitute an attractive solution. In such a context, platooning navigation appears as a desirable additional functionality, since on one hand it can improve safety and fluidity in the traffic, and on the other hand it can ease maintenance operations (e.g. to guide a group of vehicles to some station in one journey). Platooning is therefore considered in this paper and two points of special interest are investigated more particularly.

First, a manual navigation mode is considered, that is to say the lead vehicle is manually driven, defining on-line the path to be followed by the other vehicles. To deal with this problem, a first strategy consists in designing lateral and longitudinal vehicle control laws so that each vehicle tracks its direct predecessor and/or follower, see e.g. [1], [2], [3]. However, with such strategies, servoing errors are necessarily accumulated, leading when the platoon is long to unacceptable longitudinal oscillations and a growing lateral drift between the followers and the original track of the lead vehicle. To overcome these difficulties, vehicles must share a common reference trajectory and their localization must be supplied in a global coordinate system. In [4] and [5], this problem is tackled by introducing virtual rigid structures. However, they are not suited to the platoon application considered here: since some pre-specified geometric patterns are imposed, followers cannot accurately reproduce the lead vehicle trajectory. To address specifically this objective, the trajectory-based strategy proposed in [6] is considered. It is supported by inter-vehicle communications. The reference path is created on-line from the successive locations of the lead vehicle and then lateral and longitudinal control laws are designed respectively to ensure convergence to this path and to maintain a pre-specified curvilinear vehicle inter-distance.

Fig. 1. Experimental vehicles: a Cycab leading a RobuCab

The trajectory-based strategy proposed in [6] has been demonstrated with the experimental vehicles shown in Fig. 1, equipped with RTK-GPS receivers for absolute localization. However, cameras are arguably most appropriate sensors in an urban context, since they are cheap and image processing is enriched by the presence of buildings, which in contrast mask satellite signals used by GPS receivers. Therefore, the second point addressed here concerns absolute vehicle localization by monocular vision. In the literature, visual SLAM can be divided into two main approaches. The first one relies on recursive statistical techniques [7] which, though successful on the short term, suffer from error accumulation on the long term. In order for the vehicles to be supplied with a reliable localization, a monocular visual SLAM strategy, relying on a bundle adjustment [8] has been

This work is supported by the French National Research Agency (ANR) under the grant ANR-10-VPTT-011 attributed to the SafePlatoon project.

investigated in [9] in order to complete accurate automated platooning (i.e. the lead vehicle was autonomously controlled with respect to a pre-specified reference trajectory).

The objective of this paper is to extend previous work [6] and [9] in order to achieve high accuracy ***manual convoying relying on monocular vision***, i.e. the lead vehicle is this time freely driven by a human operator. To meet this aim, the slight distortions in the virtual vision world are first investigated and a local scale factor function is proposed to correct them. Next, a methodology is proposed to integrate this correction, computed along the path used to build the virtual vision world, to the reference trajectory created on-line from the lead vehicle successive positions. These two results ensure that, if a virtual vision world has been preliminary reconstructed in a set of streets, then a platoon can be manually driven freely within these streets, relying only on monocular vision, with performances similar to those achieved with an RTK GPS.

II. Overview of the Platooning Strategy

The proposed platooning strategy can be divided into 7 modules: a map of the urban environment is built beforehand via an off-line procedure, see module 1 below. A manually driven vehicle (named lead vehicle or vehicle 1) is then able to share on-line its trajectory with $n-1$ fully automated vehicles (named followers) so that these latter can accurately repeat the lead vehicle trajectory with pre-specified inter-distances. The module architecture for the lead vehicle and for the followers is described respectively in Fig. 2 and Fig. 3 and sketched in the sequel.

1. *Map reconstruction* During a preliminary step, a vehicle is manually driven within the urban environment and a video sequence as well as proprioceptive information are jointly recorded with a single camera and odometers. From the video sequence, a 3D reconstruction of the environment in the vicinity of the vehicle trajectory is then computed using a method relying on bundle adjustment, see [8], and stored in an appropriate database. The reconstructed trajectory, thereafter called *original trajectory* and denoted $\Gamma^\star$, is however defined in a non-metric virtual vision world and presents therefore distortions. An accurate localization in a metric world can nevertheless be achieved, by using corrections inferred from a non-linear observer that relies on odometric data. More details can be found in [9].

2. *Local perception* During the platooning operation, each vehicle can infer on-line its location in the virtual vision world from the data supplied by its camera and the 3D map built in module 1. Namely, $(O_i^v,\ \theta_i^v)$ is supplied on-line:
- O_i^v: coordinates of the center of the rear axle of the i^{th} vehicle, expressed in the vision world,
- θ_i^v: heading of the i^{th} vehicle in the vision world.

These data are supplemented with proprioceptive ones:
- v_i: linear velocity of the i^{th} vehicle at point O_i
- δ_i: front wheel steering angle of the i^{th} vehicle.

Details and localization performances can be found in [8].

3. *Trajectory creation* In order to serve as an objective for the followers, the successive localization data O_1^v of the lead vehicle are converted into a smooth trajectory Γ^v (named as *reference trajectory* in the sequel), extended on-line via repeated local optimizations of B-Spline curves. Such an approach had been introduced in [6], but the main exteroceptive sensor was a RTK-GPS. The validation of this trajectory creation procedure when the localization is supplied in a non-metric and distorted vision world is the first contribution of this paper, detailed in Section III-C and investigated further in Section V-.1.

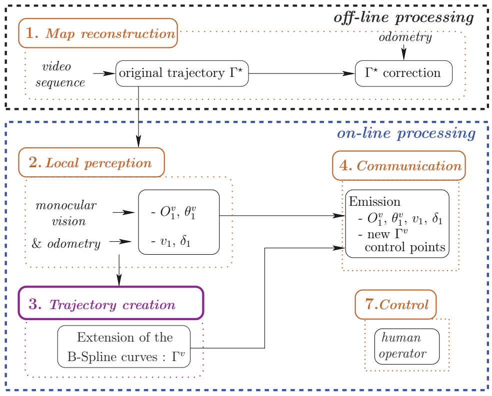

Fig. 2. Platoon architecture : lead vehicle

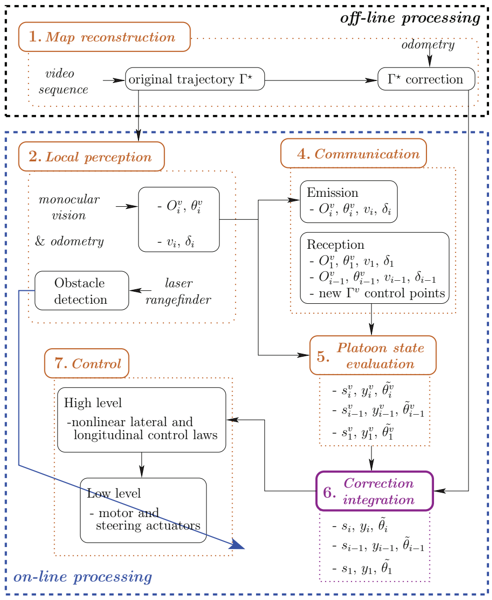

Fig. 3. Platoon architecture : i^{th} vehicle

4. *Communication* During platooning operation, on one hand the lead vehicle transmits the updated control points defining the B-Spline curve Γ^v to the followers, and on the other hand these latter receive the local perception data from both the lead vehicle and the preceding one, as well as transmit their own local perception data to their immediate follower, so that the global decentralized control strategy discussed in Section I can be implemented.

5. *Platoon state evaluation* Any data obtained asynchronously from the vehicle own sensors is timestamped. Moreover, a NTP client ensures that all the vehicles that are exchanging timestamped data via wireless communication share the same time reference. Consequently, an actualization

procedure ensuring the temporal consistency of all data can be run: at each control sample time on a given vehicle, all data are updated to that instant by simulating vehicle kinematic models on short time horizons. Finally the platoon state variables required in the global decentralized control strategy are evaluated in the virtual vision world. For the i^{th} vehicle, these variables are related to the lead vehicle, the preceding and the current one:

- $s^v_{k\in\{1,i-1,i\}}$: vehicle arc-length coordinate along Γ^v,
- $y^v_{k\in\{1,i-1,i\}}$ and $\tilde{\theta}^v_{k\in\{1,i-1,i\}}$: vehicle lateral and angular deviations with respect to. Γ^v.

6. *Correction integration* In order to ensure high accuracy platooning, platoon state variables have next to be expressed in metric world. Proper integration of the corrections, computed in module 1 along reference trajectory Γ^v, is the second contribution of this paper, presented in Section IV-B and demonstrated in Sections V-.2 and V-.3. For the i^{th} vehicle, this supplies variables $s_{k\in\{1,i-1,i\}}$, $y_{k\in\{1,i-1,i\}}$ and $\tilde{\theta}_{k\in\{1,i-1,i\}}$ expressed in metric world.

7. *Control* Relying on nonlinear control techniques, vehicle lateral and longitudinal control can be decoupled in an exact way: lateral control for the i^{th} vehicle is then designed to ensure the convergence of y_i and $\tilde{\theta}_i$ to zero, when in the nominal case longitudinal control is independently designed to regulate $s_1 - s_i$, i.e. the gap between the i^{th} vehicle and the lead one. Since each vehicle within the platoon is controlled with respect to common references (trajectory Γ^v for lateral control, lead vehicle arc-length s_1 for longitudinal control), the whole platoon can be guided without any error accumulation, so that high performances can be achieved. Nevertheless, for obvious safety reasons, if the preceding vehicle is abnormally close, the longitudinal control law is then smoothly modified to regulate $s_{i-1} - s_i$, i.e. the gap to the preceding vehicle. And if an obstacle was detected by the vehicle laser rangefinder, then longitudinal control would be overridden to avoid any collision risk. More details on control strategy, as well as performance analysis with respect to experiment reports involving up to four vehicles, are supplied in [6].

III. PRECISE LOCALIZATION FROM MONOCULAR VISION

Since the 3D reconstruction of the environment achieved in module 1 relies solely on monocular vision, the scale of the resulting virtual vision world is not properly defined. As a first step, this world can be roughly scaled by introducing a global scale factor inferred from the comparison between the total covered distance supplied by the vehicle odometers and the same quantity evaluated from vision algorithm. However slight local distortions can still be noticed, so that a localization accurate to within few centimeters, as required for control purpose, cannot alas be guaranteed. The distortion phenomenon is first highlighted in Section III-A. Next, the approach proposed in [9] to correct these distortions when the vehicle is in the vicinity of the original trajectory $\Gamma^\star$ is recalled in Section III-B. Finally, it is demonstrated in Section III-C that distortions can be handled in the same way even when vehicles are few meters apart from $\Gamma^\star$, making it possible to consider manual convoying within the urban environment reconstructed in module 1.

A. Distortion in the virtual vision world

The distortion phenomenon is illustrated in Fig.4, comparing trajectories recorded from an RTK-GPS receiver and a calibrated camera. Despite global scale factor correction, it clearly appears that the two trajectories do not properly fit.

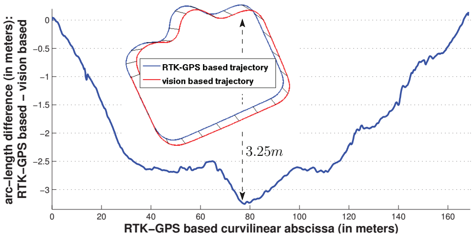

Fig. 4. Error in arc-length distance estimation with vision

To investigate distortions further, the main plot in Fig.4 shows the difference between the covered arc-length distances computed from monocular vision and from RTK-GPS data. It can be noticed that the distortion between the two worlds is largely varying, since the difference comes up to $3.25m$ in the mid-part of the trajectory. The vehicle inter-distances evaluated in the vision world are therefore inaccurate, so that high precision longitudinal control cannot be achieved if local distortions are not taken into account. The situation is different when lateral control is considered: since the sign of y^v_i and $\tilde{\theta}^v_i$ is always correct, distortions reflect as control gain variations, but lateral control objectives are still accurately achieved.

B. Accurate localization along the original trajectory $\Gamma^\star$

In previous work [9], lateral guidance along the original trajectory $\Gamma^\star$ has been carried out with several vehicles, different cameras and light conditions. It has then been shown that the distortions in the evaluation of the vehicle arc-length coordinate are definitely repeatable. Consequently, a nonlinear observer fed by vehicle odometric data has been designed to estimate a local scale factor function $\lambda^\star(s^v_i)$ attached tangentially to $\Gamma^\star$. Accurate arc-length coordinate can then be evaluated on-line as follows:

$$s_i = \int_0^{\tau(s^v_i)} \lambda^\star(\tau) \left|\left| \frac{\partial \Gamma^\star}{\partial \tau}(\tau) \right|\right| d\tau \tag{1}$$

where $\tau(s^v_i)$ is the parameter value of the 2D-curve $\Gamma^\star(\tau)$ at the arc-length coordinate s^v_i, and high accuracy longitudinal control has been demonstrated when the platoon follows a lead vehicle guided (in an automated mode) along $\Gamma^\star$.

C. Toward accurate localization along an alternative reference trajectory Γ^v

When manual convoying is considered, arc-length coordinates are no longer computed along the original trajectory $\Gamma^\star$, but along the reference trajectory Γ^v created on-line by the lead vehicle. It is shown below that distortions are locally homogeneous, so that the local scale factor function $\lambda^\star(s^v_i)$ introduced above can still be used to supply relevant inter-vehicle distances. More precisely, distortions tangentially and perpendicularly to the original trajectory $\Gamma^\star$ are investigated here. An experimental study was quite uneasy since it would have demanded for a large navigation area and for complex devices to ensure temporal consistency between the data obtained from several lateral guidance experiments at related distances from $\Gamma^\star$. For these reasons, the analysis has been conducted from simulations. The motion of a camera has been emulated in an environment consisting of textured blocks. The 3D reconstruction, shown in Fig.5 part c), has been obtained from a sequence recorded when the camera is moving in the middle of the track for four successive rounds. The distortions are attested by the spiral shape of the trajectory. Localization with respect to this trajectory has then been computed from images recorded on sequences off-centered by $4m$ on each side of the track, as presented on parts a) and b). The simple shape of the trajectory allows to adjust the camera speed and measurement intervals so that the images acquired on the off-centered trajectories can be matched temporally.

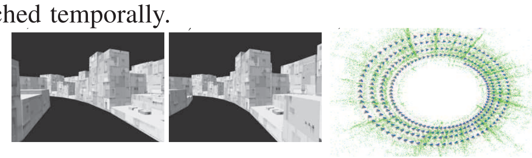

Fig. 5. a) and b) Images obtained resp. left and right w.r.t. the initial track, c) 3D reconstruction of the simulated circular environment.

The lateral component of the distortion (measured between off-centered sequences) and the tangential one (measured between two adjacent images in the same sequence) are plotted in the left part in Fig.6. It can be noticed that lateral and tangential components are similarly distorted (a linear profile is here observed because of the circular shape of the trajectory). This local homogeneity property ensures that the distances evaluated in the vision world can be corrected with solely a 1-dimensional function attached to $\Gamma^\star$. Consequently, provided that the local scale factor function $\lambda^\star(s_i^v)$ computed during the 3D map reconstruction is properly integrated, the arc-length distance along any alternative trajectory Γ^v, as well as any other vehicle variable (just as the reference trajectory curvature (required in control laws) shown in the right part in Fig.6) can be accurately evaluated on-line, enabling high performance platooning.

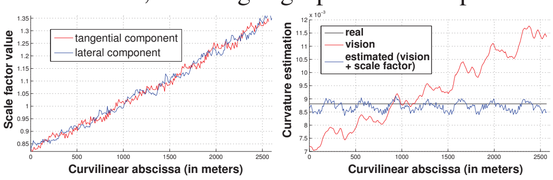

Fig. 6. Estimate of the scale factor in orthogonal directions

IV. TRAJECTORY GENERATION

Platoon state variables are expressed with respect to the reference trajectory Γ^v, which must be at least C^2 since the reference path curvature is required in control laws. To meet this requirement, it is here proposed to describe Γ^v as B-Spline curves, inferred from the set Ω of successive absolute localizations of the lead vehicle and evaluated in the virtual vision world. Since Γ^v must be as close as possible to the actual lead vehicle trajectory, the extension procedure is viewed as an optimization problem. The difficulty lies in extending Γ^v without modifying what had been previously built, in order for any variable (s_i^v, y_i^v, $\tilde{\theta}_i^v$, etc.) to keep consistent values although Γ^v is being extended. In previous work [6], this problem has been addressed when vehicle localization data were supplied by an RTK-GPS receiver. The proposed B-Spline extension process is first recalled and the way it can be extended in order to deal with vehicle localization obtained from monocular vision is then detailed.

A. B-Spline optimization

B-Spline curves consist in the concatenation of 2-dim. polynomial curves $Q^i(t) = (\, Q^i_x(t)\,,\, Q^i_y(t)\,)$, with $t \in [0,1]$. Each polynomial $Q^i(t)$ is a linear combination of basis polynomials $\{b_j(t)\}_{(0\leq j\leq d)}$ whose degree d and coefficients are selected to satisfy continuity constraints. The i^{th} B-Spline curve $Q^i(t)$ can then be expressed as:

$$Q^i(t) = \begin{pmatrix} b_0(t) & \dots & b_d(t) \end{pmatrix} \begin{pmatrix} P^i_x & P^i_y \\ \vdots & \vdots \\ P^{i+d}_x & P^{i+d}_y \end{pmatrix} \quad (2)$$

The coefficients $(\, P^k_x\,,\, P^k_y\,)_{(i\leq k\leq i+d)}$ constitute the so-called control points, that shape the B-Spline curve $Q^i(t)$. Approximating raw data Ω consists then in finding optimal values for $(\, P^k_x\,,\, P^k_y\,)$, such that each B-Spline $Q^i(t)$ fits at best with the raw trajectory Ω. In order to limit the modifications on the trajectory previously built and bound the computing time, only the most recent polynomials $Q^i(t)$ are here updated when a new localization data is available. More precisely, let n_{ac} *(as active curves)* be the number of polynomials $Q^i(t)$ entering into the optimization process, see Fig. 7. In order to freely shape n_{ac} polynomials, $n_{ap} = n_{ac} + d$ control points *(with n_{ap} as active points)* should be adjusted. The drawback of such a choice is that $n_{ac}+d$ polynomials would then be altered by the update on these control points, when the optimization criterion considers only n_{ac} polynomials. The fitting performance on the d polynomials disregarded in the optimization could then be damaged. In contrast, if only $n_{ap} = n_{ac}$ control points are adjusted, then only the n_{ac} polynomials in the optimization criterion are updated, but optimal fitting might not be reached since d control points are missing to freely shape these polynomials. The best compromise on n_{ac} and n_{ap} values has been discussed in [6] via extensive numerical simulations.

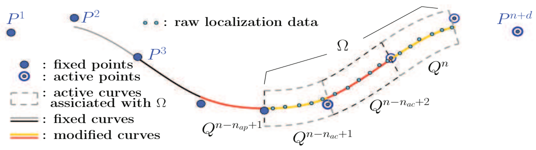

Fig. 7. B-Spline creation process with $d = 3$, $n_{ac} = 3$, $n_{ap} = 4$

Reference trajectory Γ^v is therefore built incrementally by considering a sliding optimization window on the latest localization data of the lead vehicle. Thus, when a new position O^v_1 is available, it is incorporated to Ω. When the arc-length value along the last polynomial $Q^n(t)$ is beyond a given threshold, the subset of Ω associated with $Q^{n-n_{ac}+1}(t)$ is removed from the optimization criterion and a new control point is added to the trajectory representation, introducing a new polynomial $Q^{n+1}(t)$.

B. Integration of local scale factor corrections

Since the reference trajectory Γ^v is expressed in the vision world, the local scale factor function $\lambda^\star(s_1^v)$, computed off-line during the preliminary reconstruction step (module 1), has to be properly integrated on Γ^v. At each step of the on-line extension procedure, it has to be incorporated on the last n_{ap} polynomials of Γ^v modified at this step. Since distortions have been shown to be locally homogeneous, the local scale factor value at any point P on Γ^v is chosen as the one active at point P', defined as the projection of P on $\Gamma^\star$.

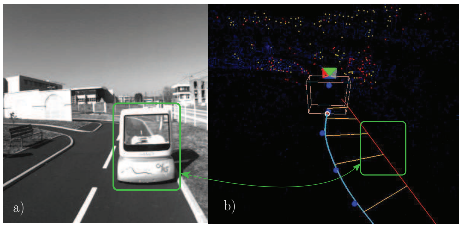

Fig. 8. a) image a short instant before the vehicle avoidance, b) vehicle representation in the 3D reconstruction

The integration of the local scale factors is illustrated in Fig.8 during the avoidance experiment described further in Section V. More precisely, the lead vehicle[1] is avoiding another one stopped on the traffic lane previously followed to record $\Gamma^\star$. The red line represents $\Gamma^\star$, when blue line and points are respectively the active B-Spline curves of Γ^v and their control points. The orange line describes the local scale factor correspondence between the current lead vehicle trajectory captured by Γ^v and the original trajectory $\Gamma^\star$.

V. Experimental results

In order to investigate the capabilities of the proposed approach, several experiments have been carried out in Clermont-Ferrand at the "PAVIN Site", an open platform devoted to urban transportation system evaluation. The experimental vehicles are shown in Fig. 1. They are electric vehicles, powered by lead-acid batteries providing 2 hours autonomy. Two *(resp. four)* passengers can travel aboard the Cycab *(resp. the RobuCab)*. Their small dimensions (length 1.90m, width 1.20m) and their maximum speed (5m.s^{-1}) are appropriate for urban environments. Vehicle localization algorithms and platoon control laws are implemented in C++ language on Pentium based computers using RTAI-Linux OS. The cameras supply visual data at a sampling frequency between 7 and 15Hz, according to the luminosity. The inter-vehicle communication is ensured via WiFi technology. Since the data of each vehicle are transmitted as soon as the localization step is completed, the communication frequency is similar to the camera one. Finally, each vehicle is also equipped with an RTK-GPS receiver, devoted exclusively to performance analysis: its information are not used to control the vehicles.

[1]see also the video :
http://www.irccyn.ec-nantes.fr/~martinet/PierreAvanzini/video_lr.mp4

The experiments have been carried out with two vehicles. The 3D reconstruction of the environment supplied to each vehicle has been built from the 170m-long trajectory shown in Fig. 9. Manual convoying has then been achieved, at a constant velocity of 1m.s^{-1}, according to three scenarii:

① close to the original trajectory $\Gamma^\star$,
② off-centered of 1m from $\Gamma^\star$,
③ close to $\Gamma^\star$, excepted to avoid a static vehicle (see Fig.8).

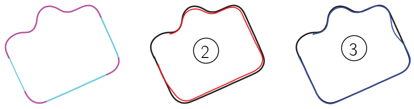

Fig. 9. Original trajectory and scenarii

1) Relevance of the corrections provided on Γ^v: For evaluation purpose, the actual local scale factors along $\Gamma^\star$ and Γ^v have been computed a posteriori, by comparing the arc-length distances obtained by monocular vision with the ones supplied by the RTK-GPS receiver. More precisely, experimental results of scenario ③ have been used and local scale factors have been evaluated on successive 2m-long segments. First, it can be observed that the profiles of the two sets of local scale factors, shown in Fig. 10, are very similar: the local homogeneity property of the distortions in the vision world, supported by simulations in Section III, is therefore corroborated experimentally.

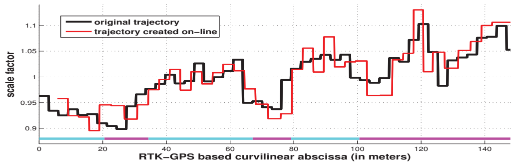

Fig. 10. Scale factor

Next, the relevance of the local scale factors attached to Γ^v, computed on-line during scenario ③, is investigated: arc-length distances along parts of Γ^v of different sizes ($6m$, $10m$ and $30m$) have been computed from raw vision data and when local scale factors computed on-line are used. Their average and maximum errors with respect to the actual arc-length distances evaluated a posteriori with the RTK-GPS sensor are compared in Fig. 11. The distances directly deduced from raw vision data are largely erroneous and their magnitude grows when the trajectory parts are longer. In contrast, when the corrections computed on-line are used, the average error is definitely smaller and no longer diverges when the trajectory parts are longer. The approach proposed to take distortions into account appears therefore relevant, even when long platoons are considered.

part length along Γ^v (m)	average error (m) raw vision	average error (m) corrected vision	maximum error (m) raw vision	maximum error (m) corrected vision
6	0.2190	0.0625	0.4792	0.1618
10	0.3391	0.0828	0.7378	0.2112
30	0.7807	0.1366	2.12	0.2257

Fig. 11. Quality of corrections provided along Γ^v

2) Relevance of the Γ^v creation procedure: The trajectories created on-line during scenarii ①, ② and ③ are investigated in Fig. 12 with respect to two criteria. For comparison purpose, the same quantities are also computed when an RTK-GPS receiver is used to create on-line the reference trajectory in scenario ②. First, the average euclidian distance between the raw data (i.e. measured vehicle locations, obtained from the camera or the RTK-GPS sensor) and their projection on the proposed reference trajectory shows that the trajectories created with a vision sensor are very satisfactory: they describe the actual trajectory of the lead vehicle to within 2cm, so that single-trace platooning can actually be achieved. Moreover, this result is very close to what can be obtained when relying on an RTK-GPS. Next, Fig. 12 displays also the average absolute variations in distance, in direction and in curvature between reference trajectories Γ^v generated at two successive iterations of the extension procedure. It can be noticed that they are all in the same range whatever the scenario and the localization sensor considered. Their quite small magnitudes demonstrate that Γ^v is smoothly extended, so that all variables required in platooning control laws (s_i^v, y_i^v, $\tilde{\theta}_i^v$, ...) keep consistent values although one extremity of Γ^v is moving.

	average error (m)	average absolute variations in distance (m)	direction (rad)	curvature (m^{-1})
vision ①	0.0165	0.0059	0.0119	0.0180
②	0.0173	0.0056	0.0102	0.0165
③	0.0172	0.0061	0.0123	0.0183
RTK-GPS	0.0089	0.0041	0.0141	0.0128

Fig. 12. Quality of the trajectory Γ^v generated on-line

3) Navigation performances: Accuracy of platooning control laws are eventually discussed. More precisely, lateral and longitudinal errors recorded from RTK-GPS measurements during scenario ③ are plotted respectively in Fig. 13 and 14. Navigation performances are however similar in the other experiments.

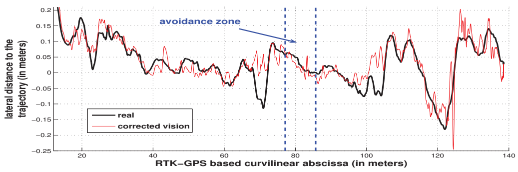

Fig. 13. follower lateral deviation

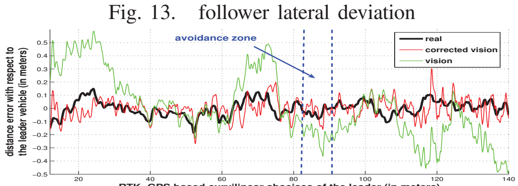

Fig. 14. longitudinal error

The lateral deviation of vehicle 2 remains mainly within ±10cm from the leader trajectory, even during the avoidance maneuver, and does not exceed 17cm during the last sinuous part of the path, see Fig. 13. Lateral guidance is therefore as satisfactory as in previous work [6], although manual convoying is here achieved relying on monocular vision instead of RTK-GPS measurements.

Inter-distance errors shown in Fig. 14 demonstrate that longitudinal control is also as accurate as previously in [6] or [9]. The local scale factors have been properly integrated into the on-line trajectory creation, so that the longitudinal error satisfactorily remains within ±10cm. In contrast, the inter-distance error computed from raw vision data, shown in green in Fig. 14, is largely erroneous: it exceeds 50cm. This demonstrates clearly the relevance of the local scale factors, even during the avoidance maneuver when vehicles are off-centered of 1.50m from the original trajectory $\Gamma^\star$.

VI. CONCLUSION AND FUTURE WORK

In this paper, manual convoying of urban vehicles has been investigated, when vehicle absolute localization is derived solely from monocular vision. The localization thus obtained is expressed in a virtual vision world slightly distorted with respect to the actual metric one. However, some properties of the distortions have been pointed out, and it has then been shown that accurate platooning can nevertheless be achieved if local scale factors are supplied. These corrections are obtained using a nonlinear observer relying only on odometric data, and can be properly integrated within the on-line extension of the reference trajectory, described as B-Spline curves. A certain freedom within the navigation space is then available, in the sense that it is possible to manually drive the platoon without being closely fastened to the trajectory used in the preliminary reconstruction step. Full scale experiments, carried out with two vehicles, have finally demonstrated the efficiency of the proposed approach. Current work is interested in on-line 3D vision world reconstruction, relying on a local bundle adjustment as proposed in [10]. It would then permit to manually convoy a platoon along any route, without requiring a preliminary reconstructed step.

REFERENCES

[1] S. Benhimane and E. Malis. Vision-based control for car platooning using homography decomposition. In *IEEE Intern. Conf. on Robotics and Automation (ICRA)*, pages 2173–2178, Barcelona (Spain), 2005.

[2] L. Consolini, F. Morbidi, D. Prattichizzo, and M. Tosques. Leader-follower formation control of nonholonomic mobile robots with input constraints. *Automatica*, 44(5):1343–1349, 2008.

[3] J.M. Contet, F. Gechter, P. Gruer, and A. Koukam. Bending virtual spring-damper: a solution to improve local platoon control. In *Intern. Conf. on Computational Science (ICCS)*, pages 601–610, Baton Rouge (USA), 2009.

[4] T. Dierks and S. Jagannathan. Control of nonholonomic mobile robot formations: backstepping kinematics into dynamics. In *IEEE Intern. Conf. on Control Applications (CCA)*, pages 94–99, Singapore, 2007.

[5] A. Gil-Pinto, P. Fraisse, and R. Zapata. Decentralized strategy for car-like robot formations. In *IEEE/RSJ Intern. Conf. on Intelligent Robots and Systems (IROS)*, pages 4176–4181, San Diego (USA), 2007.

[6] P. Avanzini, B. Thuilot, T. Dallej, P. Martinet, and J. P. Dérutin. On-line reference trajectory generation for manually convoying a platoon of automatic urban vehicles. In *IEEE/RSJ Intern. Conf. on Intelligent Robots and Systems (IROS)*, pages 1867–1872, St. Louis (USA), 2009.

[7] Andrew J. Davison. Real-time simultaneous localisation and mapping with a single camera. In *IEEE International Conference on Computer Vision, ICCV '03*, pages 1403–1410, Washington, DC, USA, 2003.

[8] E. Royer, M. Lhuillier, M. Dhome, and T. Chateau. Localization in urban environments : monocular vision compared to a differential GPS sensor. In *IEEE Conf. on Computer Vision and Pattern Recognition (CVPR)*, pages 114–121, San Diego (USA), 2005.

[9] P. Avanzini, B. Thuilot, and P. Martinet. Accurate platoon control of urban vehicles, based solely on monocular vision. In *IEEE/RSJ Intern. Conf. on Intelligent Robots and Systems (IROS)*, pages 6077–6082, Taipei (Taiwan), 2010.

[10] E. Mouragnon, M. Lhuillier, M. Dhome, F. Dekeyser, and P. Sayd. Real time localization and 3D reconstruction. *IEEE Conf. on Computer Vision and Pattern Recognition (CVPR)*, pages 363–370, 2006.